Table 3 Factors associate with emergence of LAM-resistant virus determined by multivariate analysis

	Hazard ratio	95% confidence interval	*P*-value
Gender			
0: male	1	0.497–1.455	0.55
1: female	1.176		
Age			
0: ≤50	1	0.640–1.700	0.87
1: >50	0.959		
Chronic hepatitis/liver cirrhosis			
0: CH	1	0.656–1.740	0.79
1: LC	0.935		
Pretreatment ALT (IU/L)			
0: ≤200	1	0.605–1.818	0.87
1: >200	0.953		
HBV DNA (logcopies/mL)			
0: ≤6.5	1	0.394–1.125	0.13
1: >6.5	1.502		
HBeAg			
0: negative	1	0.499–1.337	0.42
1: positive	1.225		
Combination therapy with interferon			
0: no	1	0.410–1.303	0.29
1: yes	1.368		
IBR			
0: positive	1	0.483–1.312	0.37
1: negative	1.256		
IVR			
0: positive	1	0.159–0.536	<0.001
1: negative	3.425		

HBeAg, hepatitis B e antigen; HBV, hepatitis B virus; IBR, initial biochemical response; IVR, initial viral response; LAM, lamivudine.

DISCUSSION

IN LAM THERAPY for patients with chronic HBV infection, the emergence of a LAM-resistant YMDD mutant virus is a serious problem, because it inevitably restricts the antiviral efficacy of LAM. To resolve this, detailed studies are needed to identify factors related to the emergence of the YMDD mutant virus. To date, a few investigators have suggested male gender, advanced age, high baseline ALT, the presence of severe acute exacerbation of the liver disease, high baseline HBV DNA and HBeAg-positivity as possible predictors of the emergence of LAM-resistant virus.[7,17,18] Lower body surface area was also reported as a significant factor for virological and biochemical therapeutic effect.[19] In the present study, we studied 190 patients with chronic hepatitis B treated with LAM and investigated baseline and on-treatment factors affecting the emergence of LAM-resistant mutant virus. Univariate analysis revealed that two baseline factors, high HBV DNA and HBeAg positivity, had a relation to the high incidence of the YMDD mutant virus, which is consistent with previous reports.[7,17,18] In addition, two on-treatment factors, IBR and IVR, were found to be correlated with the emergence of LAM resistance. Patients who did not show IVR had a 3.4-fold higher incidence of the emergence of the YMDD mutant virus than those who did show IVR. This agrees with a previous report that the HBV DNA level after 6 months of therapy may be a determinant for subsequent occurrence of a LAM-resistant mutant virus.[20] Multivariate analysis showed that only the absence of IVR was a significant factor contributing to the emergence of LAM-resistant virus. Baseline HBV DNA and HBeAg status were not selected as significant factors by multivariate analysis probably because of the tendency for higher HBV DNA and high frequency of HBeAg positivity in IVR-negative patients compared with IVR-positive patients. It is particularly interesting that the absence of IVR, rather than other baseline and on-treatment factors, was a powerful independent pre-

dictor for the emergence of the YMDD mutant virus in LAM therapy for chronic HBV infection. This means that IVR of an on-treatment factor is very important for good therapeutic effect and the stage for the next therapeutic strategy can thus be set in a new light with this information.

Our results showed that approximately one-seventh of the patients with chronic hepatitis B treated with LAM did not achieve IVR. In the non-IVR patients, the antiviral therapeutic regimen should be amended due to the frequent emergence of LAM-resistant virus. Recently, new nucleos(t)ide analogs have become available for the treatment of chronic HBV infection. ETV has been reported to be more effective for the reduction of HBV DNA and the less frequently induced drug-resistant mutant virus than LAM in "naïve" patients with chronic hepatitis B who had not previously received nucleos(t)ide analog therapy.[10,11] ETV was also effective in patients with chronic HBV infection showing LAM resistance,[21] but the emergence rate of the ETV-resistant virus was considerably higher in LAM-resistant patients than in naïve patients.[13,22] This is because the ETV-resistant HBV strain is established by LAM-resistant YMDD mutation plus additional mutation(s) at the amino acid position(s) 184, 202 and/or 250 within the reverse transcriptase domain of HBV.[22] According to these findings, switching from LAM to ETV may be useful for treating patients who do not achieve IVR on LAM administration. This should be done before the emergence of LAM-resistant YMDD mutant virus so as not to reduce the therapeutic efficacy of ETV. In clinical practice, there are still a number of patients who have already been on continuous LAM therapy, although the current first choice drug for patients with chronic HBV infection is ETV. In our opinion, foregoing patients without IVR or YMDD mutant viruses should be switched from LAM to ETV. The therapeutic efficacy of switching from LAM to ETV in non-IVR patients should be assessed by further study with a larger number of patients.

ADV and tenofovir disoproxil fumarate (TDF) have also been shown to exert antiviral efficacy in patients with chronic HBV infection with less frequent occurrence of drug-resistant mutant virus compared to LAM.[23] In addition, unlike the case of ETV, both ADV and TDF are known to be effective in LAM-refractory patients with chronic hepatitis B, as well as naïve patients.[23] Using ADV and TDF may be helpful for the treatment of non-IVR patients, especially after the establishment of LAM-resistant mutant virus.

In conclusion, our findings indicate that IVR may be a useful factor for predicting the emergence of LAM-resistant mutant virus in patients with chronic HBV infection treated with LAM. For patients who do not achieve IVR, therapeutic options other than LAM monotherapy should be promptly implemented because of the high incidence of the subsequent emergence of the YMDD mutant virus.

REFERENCES

1 Lavanchy D. Hepatitis B virus epidemiology, disease burden, treatment, and current and emerging prevention and control measures. *J Viral Hepat* 2004; 11: 97–107.
2 Lai CL, Chien RN, Leung NW *et al.* A one-year trial of lamivudine for chronic hepatitis B. Asia Hepatitis Lamivudine Study Group. *N Engl J Med* 1998; 339: 61–8.
3 Liaw YF, Sung JJ, Chow WC *et al.* Lamivudine for patients with chronic hepatitis B and advanced liver disease. *N Engl J Med* 2004; 351: 1521–31.
4 Papatheodoridis GV, Dimou E, Dimakopoulos K *et al.* Outcome of hepatitis B e antigen-negative chronic hepatitis B on long-term nucleos(t)ide analog therapy starting with lamivudine. *Hepatology* 2005; 42: 121–9.
5 Allen MI, Deslauriers M, Andrews CW *et al.* Identification and characterization of mutations in hepatitis B virus resistant to lamivudine. *Hepatology* 1998; 27: 1670–7.
6 Liaw YF, Chien RN, Yeh CT *et al.* Acute exacerbation and hepatitis B virus clearance after emergence of YMDD motif mutation during lamivudine therapy. *Hepatology* 1999; 30: 567–72.
7 Lai CL, Dienstag J, Schiff E *et al.* Prevalence and clinical correlates of YMDD variants during lamivudine therapy for patients with chronic hepatitis B. *Clin Infect Dis* 2003; 36: 687–96.
8 Hadziyannis SJ, Tassopoulos NC, Heathcote EJ *et al.* Adefovir dipivoxil for the treatment of hepatitis B e antigen-negative chronic hepatitis B. *N Engl J Med* 2003; 348: 800–7.
9 Marcellin P, Chang TT, Lim SG *et al.* Adefovir dipivoxil for the treatment of hepatitis B e antigen-positive chronic hepatitis B. *N Engl J Med* 2003; 348: 808–16.
10 Chang TT, Gish RG, Man RD *et al.* A comparison of entecavir and lamivudine for HBeAg-positive chronic hepatitis B. *N Engl J Med* 2006; 354: 1001–10.
11 Lai CL, Shouval D, Lok AS *et al.* Entecavir versus lamivudine for patients with HBeAg-negative chronic hepatitis B. *N Engl J Med* 2006; 354: 1011–20.
12 Hadziyannis SJ, Tassopoulos NC, Heathcote EJ *et al.* Long-term therapy with adefovir dipivoxil for HBeAg-negative chronic hepatitis B for up to 5 years. *Gastroenterology* 2006; 131: 1743–51.
13 Colonno RJ, Rose R, Baldick CJ *et al.* Entecavir resistance is rare in nucleoside naïve patients with hepatitis B. *Hepatology* 2006; 44: 1656–65.
14 Dai CY, Yu ML, Chen SC *et al.* Clinical evaluation of COBAS amplicor HBV monitor test for measuring serum

HBV DNA and comparison with the quantiplex branched DNA signal amplification assay in Taiwan. *J Clin Pathol* 2004; 57: 141–5.
15 Kamisango K, Kamogawa C, Sumi M *et al.* Quantitative detection of hepatitis B virus transcription-mediated amplification and hybridization protection assay. *J Clin Microbiol* 1999; 37: 310–14.
16 Kobayashi S, Shimada K, Suzuki H *et al.* Development of a new method for detecting a mutation in the gene encoding hepatitis B virus reverse transcriptase active site (YMDD motif). *Hepatol Res* 2000; 17: 31–42.
17 Tsubota A, Arase Y, Suzuki F *et al.* Severe acute exacerbation of liver disease may reduce or delay emergence of YMDD motif mutants in long-term lamivudine therapy for hepatitis B e antigen-positive chronic hepatitis B. *J Med Virol* 2004; 73: 7–12.
18 Chang ML, Chien RN, Yeh CT *et al.* Virus and transaminase levels determine the emergence of drug resistance during long-term lamivudine therapy in chronic hepatitis B. *J Hepatol* 2005; 43: 72–7.
19 Nakamuta M, Kotoh K, Tanabe Y *et al.* Body surface area is an independent factor contributing to the effects of lamivudine treatment. *Hepatol Res* 2005; 31: 13–17.
20 Yuen MF, Sablon E, Hui CK *et al.* Factors associated with hepatitis B virus DNA breakthrough in patients receiving prolonged lamivudine therapy. *Hepatology* 2001; 34: 785–91.
21 Sherman M, Yurdaydin C, Sollano J *et al.* Entecavir for treatment of lamivudine-refractory, HBeAg-positive chronic hepatitis B. *Gastroenterology* 2006; 130: 2039–49.
22 Tenney DJ, Rose RE, Baldick CJ *et al.* Two-year assessment of entecavir resistance in lamivudine-refractory hepatitis B virus patients reveals different clinical outcomes depending on the resistance substitutions present. *Antimicrob Agents Cheomother* 2007; 51: 902–11.
23 Bommel F, Wunsche T, Reinke P *et al.* Comparison of adefovir and tenofovir in the treatment of lamivudine-resistant hepatitis B virus infection. *Hepatology* 2004; 40: 1421–5.

Hepatology Research 2008; 38: 622–628 doi: 10.1111/j.1872-034X.2007.00307.x

Case Report

Early emergence of entecavir-resistant hepatitis B virus in a patient with hepatitis B virus/human immunodeficiency virus coinfection

Aimi Kanada,[1] Tetsuo Takehara,[1] Kazuyoshi Ohkawa,[1,2] Michio Kato,[3] Tomohide Tatsumi,[1] Takuya Miyagi,[1] Ryotaro Sakamori,[1] Shinjiro Yamaguchi,[1] Akio Uemura,[1] Keisuke Kohga,[1] Akira Sasakawa,[1] Hayato Hikita,[1] Kiyomi Kawamura,[4] Tatsuya Kanto,[1,2] Naoki Hiramatsu[1] and Norio Hayashi[1]

[1]*Department of Gastroenterology and Hepatology,* [2]*Department of Dendritic Cellular Research and Clinical Application, Osaka University Graduate School of Medicine, Yamadaoka, Suita and Departments of* [3]*Gastroenterology and* [4]*Immunology Infectious Disease, National Hospital Organization Osaka National Hospital, Hoenzaka, Chuo-ku, Osaka, Japan*

The efficacy of entecavir for patients with hepatitis B virus/human immunodeficiency virus coinfection has not been fully elucidated. Here we examined a patient coinfected with both viruses in whom entecavir-resistant hepatitis B virus appeared. The 60-year-old Japanese male with the coinfection received antiretroviral therapy including lamivudine. The therapy initially suppressed replication of both viruses, followed by reactivation of the hepatitis B virus alone by 2 years of therapy. He subsequently received entecavir therapy in addition to the antiretroviral regimen. After entecavir administration, the hepatitis B virus DNA level was slightly reduced, but then increased after 6 months of entecavir therapy. In the sequencing analysis of hepatitis B virus, no drug resistance-associated amino acid substitutions were observed in the reverse transcriptase (rt) domain before antiretroviral therapy. The lamivudine-resistant amino acid substitutions at rt173, rt180 and rt204 were detected before entecavir administration, and further the entecavir-resistant rt202 substitution was observed after 6 months of entecavir therapy. The full-length hepatitis B sequences showed that the viral strain derived from the patient belonged to genotype H. In summary, this report describes a patient with hepatitis B virus/human immunodeficiency virus coinfection who received entecavir therapy in addition to an antiretroviral regimen and showed the early emergence of entecavir-resistance hepatitis B virus. In entecavir therapy for patients infected with both viruses, great care should be taken with respect to the emergence of entecavir-resistant hepatitis B virus, especially in patients with pre-existing lamivudine-resistant virus.

Key words: coinfection, drug-resistant hepatitis B virus, entecavir, hepatitis B virus, human immunodeficiency virus, lamivudine

INTRODUCTION

CHRONIC CARRIERS OF hepatitis B virus (HBV) number more than 350 million worldwide.[1] Chronic HBV infection is seen in approximately 10% of human immunodeficiency virus (HIV)-infected patients,[2] and coinfection with HBV and HIV is a serious health problem due to the shared mode of transmission. Since the prognosis of HIV-infected patients can be dramatically improved by highly active antiretroviral therapy (HAART), one of the major causes of mortality in HIV-infected patients is chronic liver disease due to HBV infection.[3]

Lamivudine (LAM, also abbreviated to 3TC), one of the antiretroviral drugs, has also been used for the reduction of HBV replication and improvement of HBV-related liver diseases.[4,5] However, the anti-HBV effect of LAM is hampered by the emergence of LAM-resistant mutant virus in cases of HBV monoinfection and HBV/

Correspondence: Professor Norio Hayashi, Department of Gastroenterology and Hepatology, Osaka University Graduate School of Medicine, Suita 565-0871, Japan. Email: hayashin@gh.med.osaka-u.ac.jp
Received 21 August 2007; revision 31 October 2007; accepted 1 November 2007.

HIV coinfection.[6,7] The LAM-resistant HBV strain is based on point mutation occurring within the reverse transcriptase (rt) domain of the polymerase gene. A methionine-to-valine/isoleucine amino acid substitution at rt204 (rtM204V/I) is known to confer LAM resistance.[8,9] A leucine-to-methionine substitution at rt180 (rtL180M) and a valine-to-leucine substitution at rt173 (rtV173L) have also been shown to appear in association with LAM resistance.[8,10,11] The emergence rate of LAM-resistant virus in patients coinfected with HBV and HIV has been reported to be approximately 50% after 2 years of therapy.[9]

Recently, entecavir (ETV) has been reported to be superior to LAM for the suppression of viral replication and disease activity in patients with HBV monoinfection who had not received previous treatment with other anti-HBV drugs (naïve patients).[12,13] ETV has also been shown to be effective in HBV-infected patients who had been treated with LAM and showed LAM resistance.[14] It has been demonstrated that ETV resistance occurs based with amino acid substitution(s) at rt184, rt202 and/or rt250, together with the LAM-resistant rtM204V/I and rtL180M substitutions.[15] The emergence rate of ETV-resistant virus after 3 years of therapy has been reported to be less than 1% in naïve patients and 15% in LAM-resistant patients with chronic HBV monoinfection.[16] However, the anti-HBV efficacy of ETV for HBV/HIV coinfection has not been fully clarified.

In this study, we examined a patient with concomitant HBV/HIV infection who underwent HAART including LAM, and showed the appearance of LAM-resistant HBV. Subsequent ETV administration did not lead to an adequate reduction of the HBV replicative level, followed by the early emergence of the ETV-resistant virus. We investigated the serial change in the drug resistance-associated mutation status within the rt domain of the HBV polymerase gene, as well as full-length nucleotide sequences of the ETV-resistant HBV strain derived from the patient.

CASE REPORT

Patient and serum sampling

A 60-YEAR-OLD JAPANESE heterosexual male first visited to the National Hospital Organization Osaka National Hospital in December 2001 due to a positive result from an HIV antibody (anti-HIV) test in voluntary HIV screening. From his anamnestic record, he had been admitted with type B acute hepatitis to another hospital 3 years earlier. Anti-HIV had been negative at that time. On his first visit, the anti-HIV positivity was confirmed by Western blot analysis. Antibodies to HIV-1 proteins, gp160, gp110/120, p68, p52, gp41, p40 and p34 were positive. As for antibodies to HIV-2 proteins, only an antibody to p68 was positive. According to these, he was judged to be infected with HIV-1. The HIV-RNA level was $10^{4.3}$ copies/mL, and the CD4+ T cell counts were 275/mm^3 (normal range, >300/mm^3). He tested positive for hepatitis B surface antigen (HBsAg) and hepatitis B e antigen (HBeAg), and negative for antibody to HBsAg (anti-HBs) and antibody to HBeAg (anti-HBe). The HBV-DNA level was $>10^{7.6}$ copies/mL, and the alanine aminotransferase (ALT) level was 106 IU/L. The patient was free of HIV-related symptoms and had no opportunistic infectious diseases. HAART with LAM (300 mg/day), zidovudine (AZT) (600 mg/day) and efavirenz (EFV) (600 mg/day) was started in April 2002. AZT and EFV were then substituted for sanilvudine (d4T) (60 mg/day) and avacavir (ABC) (600 mg/day) in July 2002 because of anemia and dizziness. By July 2002, HIV-RNA decreased to below the detection limit ($<10^{1.7}$ copies/mL), whereas the CD4+ T cell counts tended to rise up to >500/mm^3. In August 2006, fosamprenavir (FPV) (2400 mg/day) was commenced in place of d4T due to peripheral nerve palsy. Suppression of HIV-RNA below the detection limit continued at the end of follow-up, irrespective of repeated alterations in the therapeutic regimen of HAART. As for HBV status, HBV-DNA declined to $10^{3.9}$ copies/mL in April 2003 but increased again to $>10^{7.6}$ copies/mL in May 2005. To control HBV replication, ETV (0.5 mg/day) was added in October 2006. After the ETV administration, HBV-DNA slightly decreased from $>10^{7.6}$ to $10^{6.2}$ copies/mL in January 2007 but rose to $10^{7.2}$ copies/mL 3 months later. ALT remained abnormal and HBeAg continued to be positive throughout the follow-up period. The clinical course of the patient is summarized in Figure 1a.

For the nucleotide sequencing of HBV-DNA, the serum samples were obtained in December 2001 (before HAART), August 2006 (before ETV administration), and April 2007 (after 6 months of ETV therapy). These serum sampling points were designated as P1, P2 and P3 (see Fig. 1a). Serum samples were stored at −80°C until use. Informed consent was obtained from the patient.

Virus markers and nucleotide sequencing

HBsAg, anti-HBs, HBeAg, anti-HBe and anti-HIV were tested by chemiluminescent immunoassay. A

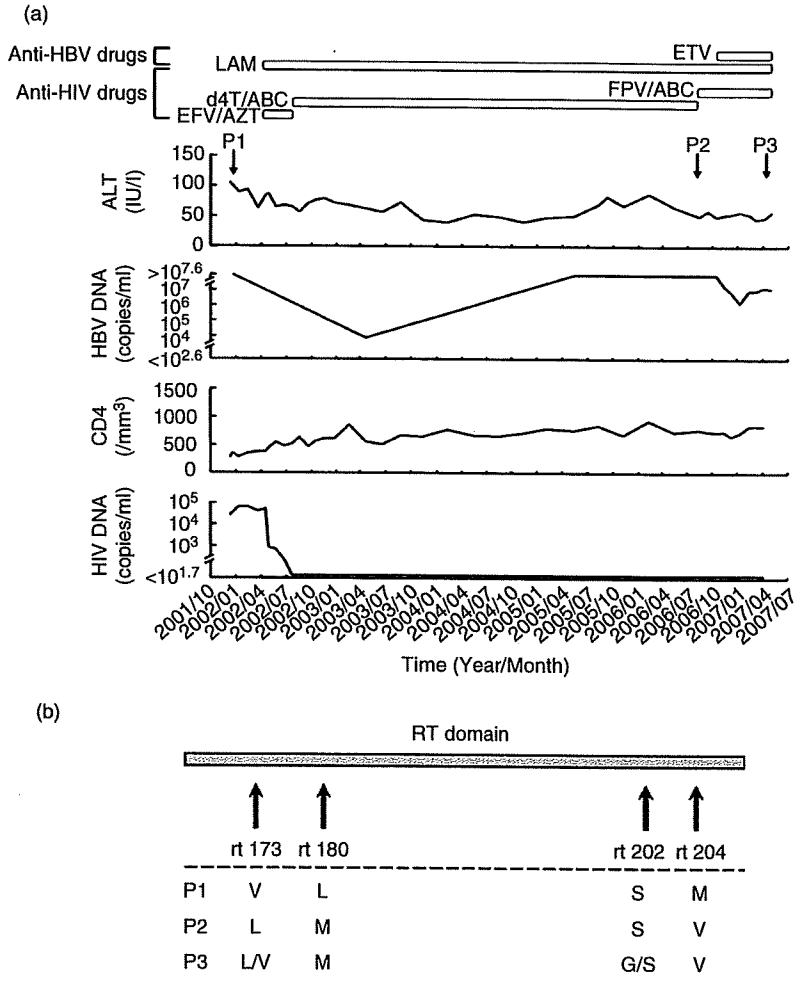

Figure 1 (a) Patient clinical course and serum sampling points. P1, P2 and P3 are the points at which serum samples were obtained. P1 was taken in December 2001 (before HAART), P2 in August 2006 (before ETV administration) and P3 in April 2007 (after 6 months of ETV therapy). ABC, avacavir; ALT, alanine aminotransferase; AZT, zidovudine; d4T, sanilvudine; EFV, efavirenz; ETV, entecavir; FPV, fosamprenavir; HBV, hepatitis B virus; HIV, human immunodeficiency virus; LAM, lamivudine. (b) Serial change in the status of drug resistance-associated amino acid substitutions.

confirmatory anti-HIV-1/2 testing was carried out by Western blot analysis. Serum HBV-DNA was detected by means of a PCR assay (Amplicor HB monitor; Roche Diagnostics, Basel, Switzerland) with a lower detection limit of $10^{2.6}$ (=400) copies/mL. Plasma HIV-RNA was quantified by a PCR assay (Amplicor HIV-1 monitor; Roche) whose lower detection limit was $10^{1.7}$ (=50) copies/mL.

The nucleotide sequences of HBV-DNA were determined by a method based on nested PCR and direct sequencing, as described elsewhere.[17] In this study, primers BF5-2 (5′-TCC TCA GGC CAT GCA GTG GA-3′, nt 3201-20) and BR8 (5′-TTG CGT CAG CAA ACA CTT GG-3′, nt 1195-76) were also used. Nucleotide sequences of the entire rt domain in the polymerase gene were examined in HBV strains derived from the P1 and P2 serum samples (GenBank accession nos. AB353765 and AB353766), whereas the full-length HBV-DNA was determined in the strain derived from the P3 serum sample (GenBank accession no. AB353764). The full-length HBV strain obtained in this study (designated as HBDI03), the seven representative HBV strains of genotypes A–G and the eight previously isolated HBV strains of genotype H were aligned, and the phylogenetic tree was constructed. These analyses were done at the homepage of the DNA Data Bank of Japan (http://www.ddbj.nig.ac.jp).

Results of sequencing analysis of HBV

The serial change in the nucleotide sequences in the rt domain of the HBV polymerase gene was first examined

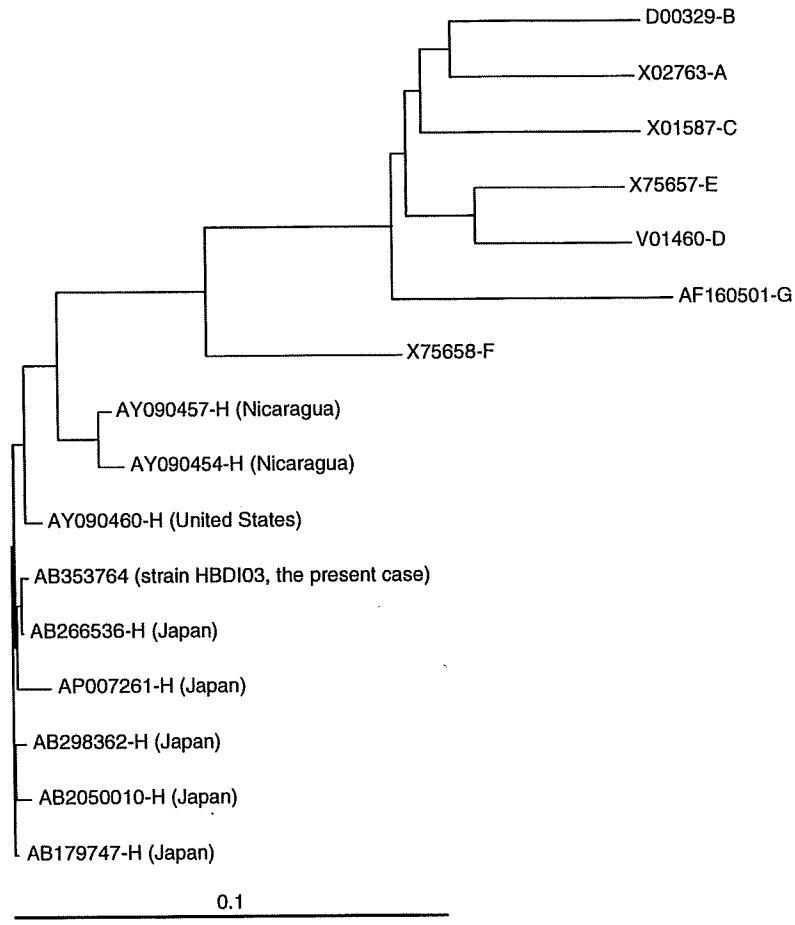

Figure 2 Phylogenetic tree analysis including the HBV strain HBDI03 obtained in this study, the seven representative HBV strains of genotypes A–G, and the eight previously isolated HBV strains of genotype H.

using serum samples obtained at P1–P3 (Fig. 1b). At point P1, no drug resistance-associated mutations were found in the rt domain, but three LAM resistance-associated substitutions, rtM204V, rtL180M and rtV173L, emerged at point P2. A serine-to-glycine substitution at rt202 (rtS202G), which has been shown to be one of the ETV resistance-associated substitutions,[15] was further observed at point P3, although rtS202G and rtV173L substitutions occurred incompletely. No other amino acid substitutions were seen in the rt domain of the HBV polymerase gene from point P1 to P3. Thus, in the patient with HBV/HIV coinfection, the emergence of the drug resistance-associated amino acid substitutions revealed a close relationship with the poor anti-HBV efficacy of LAM and ETV.

Next, the full-length nucleotide sequences of HBV were determined from the P3 serum sample of the patient with HBV/HIV coinfection showing ETV resistance. The full-length HBV strain HBDI03 comprised a total of 3215 nucleotide lengths. The phylogenetic tree was depicted using the HBV strain HBDI03, the seven representative HBV strains of genotypes A–G and the eight previously identified genotype H HBV strains. As shown in Figure 2, the HBV strain HBDI03 obtained in this study was classified as genotype H. When the nucleotide sequences of the strain HBDI03 were compared with the eight reported genotype H HBV strains, the strain HBDI03 showed a 97.2–99.8% identity with these strains. The unique amino acid substitutions in the strain HBDI03 were further investigated in comparison with these eight genotype H HBV strains. As shown in Table 1, four drug resistance-associated substitutions within the rt domain were observed, as described above. The two amino acid substitutions in the S gene were also caused by the same mutations of the drug resistance-associated rtV173L and rtM204V

Table 1 The unique amino acid substitutions in strain HBDI03 in comparison with eight previously isolated genotype H hepatitis B virus strains

Amino acid position	Consensus residue of genotype H	Residue unique to strain HBDI03
Polymerase		
519 (rt173)	V	L/V
526 (rt180)	L	M
548 (rt202)	S	G/S
550 (rt204)	M	V
Surface		
164	E	D/E
195	I	M
X		
32	W	G

Consensus residues of genotype H were from the eight reported hepatitis B virus (HBV) strains (GenBank accession nos. AY090454, AY090457, AY090460, AP007261, AB179747, AB205010, AB266536 and AB298362).

changes. As for the remaining one amino acid substitution in the X gene, the substituted glycine residue observed in the HBDI03 strain was a common one in the representative HBV strains of genotypes A–G at the corresponding codon position. Taken together, the HBDI03 strain did not appear to have any distinctive features other than the presence of the drug-associated amino acid substitutions.

DISCUSSION

RECENTLY, ETV HAS been widely accepted as an effective drug for the treatment of HBV monoinfection because of its stronger inhibitory effect on HBV replication and lower emergence rate of drug-resistant mutant virus compared to LAM.[12–14] ETV-resistant HBV has been demonstrated to be established by amino acid substitution(s) at rt184, rt202 and/or rt250, in addition to the LAM-resistant rtM204V/I and rtL180M substitutions.[15] The emergence rate of ETV-resistant virus has been reported to be higher in LAM-resistant patients than in naïve patients.[16] There has so far been little evidence concerning the anti-HBV efficacy of ETV for patients with HBV/HIV coinfection. In particular, LAM-resistant HBV has been shown to emerge frequently in patients with HBV/HIV coinfection who received LAM therapy as a component of HAART.[7] The therapeutic efficacy of ETV on LAM-resistant HBV should be assessed in patients with HBV/HIV coinfection. In this study, we examined a patient with HBV/HIV coinfection who had LAM-resistant HBV induced by HAART including LAM, and underwent subsequent ETV therapy. The patient showed a rather weak suppressive effect of ETV on HBV replication, followed by the emergence of ETV-resistant HBV in the early phase of therapy.

In the sequence analysis of the HBV genome, no drug-resistant HBV mutations were detected before HAART, but continuous LAM administration induced the LAM-resistant mutant HBV with rtM204V, rtL180M and rtV173L amino acid substitutions. Subsequent ETV therapy resulted in the emergence of an ETV-resistant virus possessing the rtS202G substitution in addition to the three LAM resistance-associated substitutions after no more than 6 months of ETV therapy, although the rtS202G and rtV173L substitutions were incomplete. In LAM-resistant patients with HBV monoinfection, the emergence rate of the ETV-resistant mutation has been reported to be merely 15% after 3 years of therapy.[16] In comparison with this, ETV-resistant HBV appeared in an extremely early phase of therapy in our patient with HBV/HIV coinfection. According to this, ETV resistance is speculated to be established earlier in patients with HBV/HIV coinfection than in those with HBV monoinfection, although concomitant HIV infection has not thus far been suggested to result in a higher incidence of the drug-resistant HBV strain in the treatment with other anti-HBV drugs in chronic HBV infection. The latent immune deficiency caused by HIV infection might prevent HBV eradication through a host immune response, resulting in poor anti-HBV efficacy of ETV. Alternatively, simultaneous usage of multiple antiretroviral drugs might in some way contribute to the emergence of ETV-resistant HBV.

Very recently, it has been shown that ETV possesses modest anti-HIV activity both *in vitro* and *in vivo* and can induce the drug-resistant mutant HIV strain in patients with HBV/HIV coinfection.[18] This suggests that ETV may not be appropriate for the treatment of patients with HBV/HIV coinfection in whom HAART is not needed. On the other hand, ETV is considered to be beneficial for patients with HBV/HIV coinfection undergoing a stable continuation of HAART. In particular, the therapeutic efficacy of ETV may be more promising in patients without LAM-resistant HBV than in those with it. Although the present case of the patient under discussion, who already displayed LAM-resistant HBV due to the preceding HAART, did not support the usefulness of ETV therapy because of the early emergence of ETV-resistant HBV, further studies with a large number of

patients should be completed to assess the antiviral efficacy and deliberate clinical application of ETV therapy for HBV/HIV coinfection.

Both adefovir dipivoxil (ADV) and tenofovir disoproxil fumarate (TDF) have recently been shown to effectively inhibit HBV replication in patients with HBV/HIV coinfection, irrespective of LAM resistance.[19,20] ADV exerts only anti-HBV activity and is available for patients with HBV/HIV coinfection who have no need for HAART or who are receiving a stable HAART regimen. In contrast, TDF can be used as a component of HAART because of its valuable antiviral activity against both HBV and HIV. Accordingly, ADV and TDF are currently useful drugs for patients with HBV/HIV coinfection and may be subsequent therapeutic options for the patient reported in this study.

Our patient was found to be infected with HBV of genotype H, a globally rare genotype. To date, the full-length sequences of eight genotype H HBV strains have been reported from the USA, Nicaragua and Japan (see Fig. 2). Of them, one strain has been obtained from a Japanese patient with chronic HBV monoinfection who underwent ETV therapy as a naïve patient and showed ETV resistance later.[21] The relevance of the genotype frequency to the therapeutic efficacy of ETV should be studied extensively in HBV-infected patients treated with ETV.

In Japan, genotypes B and C are prevalent in chronic HBV carriers who acquire the infection mainly through the mother-to-child transmission route. In contrast, the foreign HBV strains other than genotypes B and C have been shown to be involved in a considerable proportion of patients with acute HBV infection.[22] Infection of such foreign types of HBV possibly occurs through sexual contacts in Japan. In our patient with HBV/HIV coinfection who had genotype H HBV of foreign origin, it is speculated that acute HBV infection occurring 3 years before his first visit led to the transition to chronicity. The time of HIV infection cannot be defined due to the lack of HIV-RNA testing during the period of acute HBV infection. The possibility of simultaneous infection with HBV and HIV cannot be excluded, despite the negative result of anti-HIV at that time, because the test may have taken place during the immunological window period of HIV infection.

In summary, we have introduced a patient with HBV/HIV coinfection who underwent ETV therapy in addition to the HAART regimen and showed ETV resistance in the early phase of therapy. Our finding suggests that, in ETV therapy for patients with HBV/HIV infection, great care should be taken against the emergence of ETV-resistant HBV, especially in patients with pre-existing LAM-resistant HBV.

REFERENCES

1 Lee WM. Hepatitis B virus infection. *N Engl J Med* 1997; 337: 1733–45.
2 Konopnicki D, Mocroft A, de Wit S *et al.* EuroSIDA Group. Hepatitis B and HIV: prevalence, AIDS progression, response to highly active antiretroviral therapy and increased mortality in the EuroSIDA cohort. *AIDS* 2005; 19: 593–601.
3 Thio CL, Seaberg EC, Skolasky R Jr *et al.* Multicenter AIDS Cohort Study. HIV-1, hepatitis B virus, and risk of liver-related mortality in the Multicenter Cohort Study (MACS). *Lancet* 2002; 360: 1921–6.
4 Lai CL, Chien RN, Leung NW *et al.* A one-year trial of lamivudine for chronic hepatitis B. Asia Hepatitis Lamivudine Study Group. *N Engl J Med* 1998; 339: 61–8.
5 Benhamou Y, Katlama C, Lunel F *et al.* Effects of lamivudine on replication of hepatitis B virus in HIV-infected men. *Ann Intern Med* 1996; 125: 705–12.
6 Lai CL, Dienstag J, Schiff E *et al.* Prevalence and clinical correlates of YMDD variants during lamivudine therapy for patients with chronic hepatitis B. *Clin Infect Dis* 2003; 36: 687–96.
7 Benhamou Y, Bochet M, Thibault V *et al.* Long-term incidence of hepatitis B virus resistance to lamivudine in human immunodeficiency virus-infected patients. *Hepatology* 1999; 30: 1302–6.
8 Allen MI, Deslauriers M, Andrews CW *et al.* Identification and characterization of mutations in hepatitis B virus resistant to lamivudine. Lamivudine Clinical Investigation Group. *Hepatology* 1998; 27: 1670–7.
9 Ono-Nita SK, Kato N, Shiratori Y *et al.* Susceptibility of lamivudine-resistant hepatitis B virus to other reverse transcriptase inhibitors. *J Clin Invest* 1999; 103: 1635–40.
10 Ono SK, Kato N, Shiratori Y *et al.* The polymerase L528M mutation cooperates with nucleotide binding-site mutations, increasing hepatitis B virus replication and drug resistance. *J Clin Invest* 2001; 107: 449–55.
11 Delaney WE, Yang H, Westland CE *et al.* The hepatitis B virus polymerase mutation rtV173L is selected during lamivudine therapy and enhances viral replication in vitro. *J Virol* 2003; 77: 11833–41.
12 Chang TT, Gish RG, de Man R *et al.* BEHoLD AI463022 Study Group. A comparison of entecavir and lamivudine for HBeAg-positive chronic hepatitis B. *N Engl J Med* 2006; 354: 1001–10.
13 Lai CL, Shouval D, Lok AS *et al.* BEHoLD AI463027 Study Group. Entecavir versus lamivudine for patients with HBeAg-negative chronic hepatitis B. *N Engl J Med* 2006; 354: 1011–20.
14 Sherman M, Yurdaydin C, Sollano J *et al.* AI463026 BEHoLD Study Group. Entecavir for treatment of

lamivudine-refractory, HBeAg-positive chronic hepatitis B. *Gastroenterology* 2006; 130: 2039–49.
15 Tenney DJ, Rose RE, Baldick CJ *et al.* Two-year assessment of entecavir resistance in Lamivudine-refractory hepatitis B virus patients reveals different clinical outcomes depending on the resistance substitutions present. *Antimicrob Agents Chemother* 2007; 51: 902–11.
16 Colonno RJ, Rose R, Pokornowski K *et al.* Assessment at three years shows barrier to resistance is maintained in entecavir-treated nucleoside-naïve patients while resistance emergence increases over time in lamivudine refractory patients. *Hepatology* 2007; 44: 229A (Abstract).
17 Kanada A, Takehara T, Ohkawa K *et al.* Type B fulminant hepatitis is closely associated with a highly mutated hepatitis B virus strain. *Intervirology* 2007; 50: 394–401.
18 McMahon MA, Jilek BL, Brennan TP *et al.* The HBV drug entecavir – Effects on HIV-1 replication and resistance. *N Engl J Med* 2007; 356: 2614–21.
19 Benhamou Y, Thibault V, Vig P *et al.* Safety and efficacy of adefovir dipivoxil in patients infected with lamivudine-resistant hepatitis B and HIV-1. *J Hepatol* 2006; 44: 62–7.
20 Benhamou Y, Fleury H, Trimoulet P *et al.* TECOVIR Study Group. Anti-hepatitis B virus efficacy of tenofovir disoproxil fumarate in HIV-infected patients. *Hepatology* 2006; 43: 548–55.
21 Suzuki F, Akuta N, Suzuki Y *et al.* Selection of a virus strain resistant to entecavir in a nucleoside-naïve patient with hepatitis B of genotype H. *J Clin Virol* 2007; 39: 149–52.
22 Ozasa A, Tanaka Y, Orito E *et al.* Influence of genotypes and precore mutations on fulminant or chronic outcome of acute hepatitis B virus infection. *Hepatology* 2006; 44: 326–34.

Published June 30, 2008

JEM

ARTICLE

Length-dependent recognition of double-stranded ribonucleic acids by retinoic acid–inducible gene-I and melanoma differentiation–associated gene 5

Hiroki Kato,[1,2] Osamu Takeuchi,[1,2] Eriko Mikamo-Satoh,[3,4] Reiko Hirai,[5] Tomoji Kawai,[3] Kazufumi Matsushita,[1,2] Akane Hiiragi,[6] Terence S. Dermody,[7] Takashi Fujita,[5,6] and Shizuo Akira[1,2]

[1]Laboratory of Host Defense, World Premiere International Immunology Frontier Research Center, [2]Research Institute for Microbial Diseases, [3]Institute for Scientific and Industrial Research, Osaka University, Suita, Osaka 565-0871, Japan
[4]Department of Pharmacy, Hyogo University of Health Sciences, Cyuo-ku, Kobe, Hyogo 650-8530, Japan
[5]Laboratory of Molecular Genetics, Institute for Virus Research, and [6]Laboratory of Molecular Cell Biology, Graduate School of Biostudies, Kyoto University, Kyoto 606-8502, Japan
[7]Department of Pediatrics, Vanderbilt University School of Medicine, Nashville, TN 37232

The ribonucleic acid (RNA) helicases retinoic acid-inducible gene-I (RIG-I) and melanoma differentiation–associated gene 5 (MDA5) recognize distinct viral and synthetic RNAs, leading to the production of interferons. Although 5′-triphosphate single-stranded RNA is a RIG-I ligand, the role of RIG-I and MDA5 in double-stranded (ds) RNA recognition remains to be characterized. In this study, we show that the length of dsRNA is important for differential recognition by RIG-I and MDA5. The MDA5 ligand, polyinosinic-polycytidylic acid, was converted to a RIG-I ligand after shortening of the dsRNA length. In addition, viral dsRNAs differentially activated RIG-I and MDA5, depending on their length. Vesicular stomatitis virus infection generated dsRNA, which is responsible for RIG-I–mediated recognition. Collectively, RIG-I detects dsRNAs without a 5′-triphosphate end, and RIG-I and MDA5 selectively recognize short and long dsRNAs, respectively.

CORRESPONDENCE
Shizuo Akira:
sakira@biken.osaka-u.ac.jp

Abbreviations used in this paper: AFM, atomic force microscope; CARD, caspase-recruitment domain; cDC, conventional DC; CIAP, calf intestine alkaline phosphatase; DI, defective interfering; dsRNA, double-stranded RNA; EMCV, encephalomyocarditis virus; IPS-1, IFN-β stimulator-1; MEF, mouse embryonic fibroblast; MDA5, melanoma differentiation–associated gene 5; pDC, plasmacytoid DC; PNPase, polynucleotide phosphorylase; poly I:C, polyinosine-polycytidylic acid; PRR, pattern recognition receptor; RIG-I, retinoic acid-inducible gene-I; RLH, RIG-I–like helicase; ssRNA, single-stranded RNA; TIR, Toll/IL-1 receptor homology; TLR, Toll-like receptor; VSV, vesicular stomatitis virus.

The first line of defense against RNA virus infection relies on the innate immune system, which is initiated by the detection of viral components. Sensing of pathogens by innate immunity is mediated by host pattern recognition receptors (PRRs) that detect pathogen-specific molecular patterns (1). Three different classes of PRRs have been identified: Toll-like receptors (TLRs), retinoic acid–inducible gene-I (RIG-I)–like helicases (RLHs), and NOD-like receptors (2–4). The recognition of viruses by the PRRs leads to production of proinflammatory cytokines and type I IFNs. In particular, type I IFNs, comprised of multiple IFN-αs and -βs, are important for eliminating invading viruses by inducing death of infected cells, conferring resistance to viral infection on surrounding cells, and activating acquired immune responses.

Among PRRs, TLRs and RLHs are known to recognize viral infection. TLRs are transmembrane receptors with leucine-rich repeats and a cytoplasmic Toll/IL-1 receptor homology (TIR) domain. TLR3, 7, and 9 are located on endosome/ER membranes, and detect double-stranded (ds) RNA, single-stranded (ss) RNA, and DNA with a CpG motif, respectively (5–8). Upon encountering their cognate ligands, TLRs activate intracellular signaling cascades by recruiting the TIR domain containing adaptor molecules, such as MyD88 and TRIF (9, 10). Ultimately, the signaling leads to the expression of type I IFNs and proinflammatory cytokine genes. TLR7 and 9 are highly expressed on plasmacytoid DCs (pDCs), a cell type known to produce vast amounts of type I IFNs in response to viral infection (11). The importance of TLRs in the production of type I IFNs in pDCs have been shown by using mice deficient in MyD88, which is responsible for TLR7 and 9 signaling.

However, TLRs are dispensable for virus-induced IFN production in cell types other than pDCs. Instead, RIG-I family cytoplasmic

The online version of this article contains supplemental material.

J. Exp. Med. Vol. 205 No. 7 1601-1610 www.jem.org/cgi/doi/10.1084/jem.20080091

Published June 30, 2008

RNA helicases play a key role in sensing RNA virus invasion. The RIG-I family consists of three helicases, RIG-I, melanoma-differentiation–associated gene 5 (MDA5), and LGP2 (12–14). RIG-I and MDA5 contain two caspase-recruitment domains (CARDs) and a DExD/H-box helicase domain. The helicase domains of RIG-I and MDA5 recognize viral RNAs, and their CARDs are responsible for signaling through interacting with a CARD-containing adaptor, IFN-β promoter stimulator-1 (IPS-1) (15, 16), also called MAVS, CARDIF, and VISA (17–20), which is located in the outer mitochondrial membrane. This interaction finally activates several transcriptional factors, IFN regulator factor 3, IFN regulator factor 7, and NF-κB for the induction of type I IFNs and proinflammatory cytokines (21, 22). In contrast, LGP2 does not possess a CARD, but only a DExD/H-box helicase domain, and has been reported to function as a negative regulator (14, 23), especially of the RIG-I–mediated pathway (24, 25).

Recent studies have demonstrated that RIG-I and MDA5 are differentially involved in antiviral responses. Picornaviruses, such as encephalomyocarditis virus (EMCV), are specifically recognized by MDA5, whereas RIG-I recognizes a wide variety of RNA viruses belonging to the paramyxovirus and rhabdovirus families, as well as Japanese encephalitis virus (26). Some viruses such as Dengue virus and reovirus were shown to be recognized by both RIG-I and MDA5 (27). These two helicases have also been shown to recognize distinct types of RNAs. Single-stranded (ss) RNA with 5′-triphosphate has been identified as a RIG-I ligand (26, 28–30). The cellar 5′-triphosphate ssRNA does not exist in the cytoplasm, but in the nucleus, and ssRNAs in the cytoplasm are normally capped or processed. Thus, RIG-I can distinguish viral RNAs from vast amounts of cellar RNAs. On the other hand, small dsRNAs (ranging from 21 to 27 nucleotides) have also been reported to induce IFN-inducible genes via both ATPase and helicase activities of RIG-I (31).

However, whether or not dsRNA is also a RIG-I ligand, in addition to 5′-triphosphate ssRNA, is still controversial. Although polyinosinic-polycytidylic acid (poly I:C), an artificial double-stranded (ds) RNA, was found to be a ligand for MDA5 (26, 28), the motif recognized by MDA5 should be characterized, and a natural ligand for MDA5 is also yet to be discovered.

In this study, we investigated how RIG-I and MDA5 differentially recognize RNAs by chemically modifying poly I:C. We found that the MDA5 ligand, poly I:C, was converted to a RIG-I ligand after shortening of the dsRNA length. RIG-I and MDA5 preferentially bind to short and long poly I:Cs, respectively. In addition, dsRNAs prepared from viruses differentially activated RIG-I and MDA5, depending on the length. Whereas influenza virus infection failed to generate dsRNA in the infected cells, vesicular stomatitis virus (VSV) infection generated dsRNA, which is responsible for RIG-I–mediated recognition. Collectively, RIG-I detects dsRNAs without a 5′-triphosphate end, and RIG-I and MDA5 selectively recognize short and long dsRNAs, respectively.

RESULTS

The switching of poly I:C from an MDA5 ligand to a RIG-I ligand

We first estimated the length of the MDA5 ligand poly I:C by agarose gel electrophoresis and found that untreated poly I:C migrated as a smeared band corresponding to the mobility of ~4–8 kbp dsDNA fragments (Fig. 1 A). To analyze the importance of poly I:C length in IFN-inducing activity, we partially digested poly I:C with a dsRNA-specific endonuclease, RNase III. The size of the poly I:C became shorter in a digestion time-dependent manner, and the median size of 60 min–treated poly I:C corresponded to 300 bp dsDNA (Fig. 1 A). When WT, *Rig-I*$^{-/-}$, *Mda5*$^{-/-}$, *Rig-I*$^{-/-}$*Mda5*$^{-/-}$ mouse embryonic fibroblasts (MEFs) were stimulated with untreated poly I:C, IFN-β was induced in an MDA5-dependent manner that was consistent with previous reports (26, 28). Surprisingly, IFN-β induction by poly I:C treated with RNase III for 60 min depended on RIG-I, but not on MDA5 (Fig. 1 B). However, complete digestion of poly I:C by 180-min treatment with RNase III produced 10–20 nt dsRNA that failed to activate even wild-type cells (Fig. 1 B and unpublished data). When cells were stimulated with poly I:C partially digested for different periods, *Mda5*$^{-/-}$ MEFs gained the ability to respond to RNase III–treated poly I:C as the digestion proceeded, whereas *Rig-I*$^{-/-}$ MEFs gradually lost the ability to produce IFN-β in response to shortened poly I:C (Fig. 1 C). In addition, conventional DCs derived from bone marrow or prepared from spleen from *Rig-I*$^{-/-}$ and *Mda5*$^{-/-}$ mice also

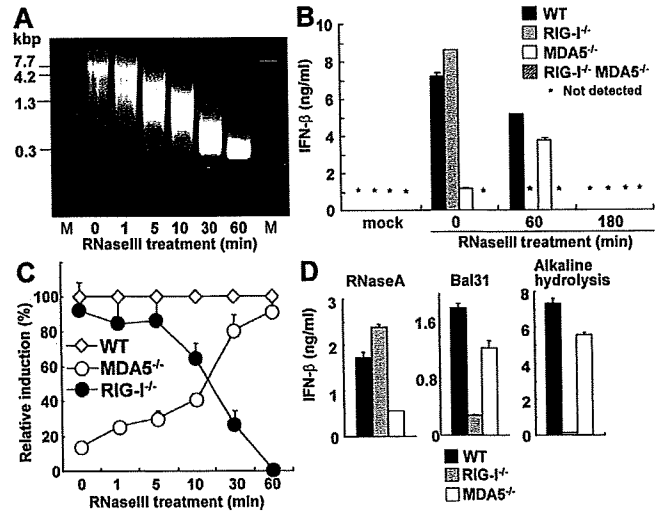

Figure 1. Preferential recognition of long and short poly I:C by MDA5 and RIG-I. (A) The indicated RNAs are shown on the ethidium bromide–stained agarose gel. M, DNA marker. (B) WT, *Rig-I*$^{-/-}$, *Mda5*$^{-/-}$, and *Rig-I*$^{-/-}$*Mda5*$^{-/-}$ MEFs were treated with 1 μg/ml of untreated or RNase III–treated poly I:C for 16 h. The production of IFN-β in the supernatant was measured by ELISA. mock, no RNA. (C) Relative induction of IFN-β after stimulation with poly I:C treated with RNase III for the indicated periods. (D) The production level of IFN-β in the stimulation with RNase A–treated, Bal31-treated, or alkaline-hydrolyzed poly I:C. Error bars show the SDs between triplicates.

Published June 30, 2008

failed to produce IFN-β in response to RNase III–digested and undigested poly I:C, respectively (Fig. S1, available at http://www.jem.org/cgi/content/full/jem.20080091/DC1). Furthermore, production of IFN-β in the sera in response to digested and undigested poly I:C conjugated with a transfection reagent was dependent on the presence of RIG-I and MDA5, respectively (Fig. S2). These results indicate the switching of poly I:C from being an MDA5 ligand to being a RIG-I ligand after partial digestion with RNase III.

Poly I:C partially digested with human Dicer also induced IFN-β in a RIG-I–dependent manner (unpublished data), indicating that this phenomenon is not specific to bacterial RNase III. In contrast, digestion of poly I:C with a ssRNA-specific nuclease, RNase A, did not affect its recognition by MDA5 (Fig. 1 D), suggesting that the shortening of the dsRNA part of poly I:C is necessary for the conversion from an MDA5 ligand to a RIG-I ligand. Consistent with the aforementioned observations, treatment with Bal 31, which degrades ssRNA and linear duplex RNA progressively from both the 5′- and 3′-ends, as well as alkaline hydrolysis, also converted poly I:C to a RIG-I ligand (Fig. 1 D). Poly I:C is an artificial dsRNA generated by annealing poly I and poly C. Poly I and C are synthesized by a bacterial enzyme, polynucleotide phosphorylase (PNPase), which catalyzes the polymerization of nucleotide diphosphate (32). Because poly I and C are synthesized with inositol diphosphate and cytidine diphosphate as substrates, poly I:C does not contain a 5′-triphosphate nucleotide, and dsRNA fragments generated by RNase III digestion contain a 5′-monophosphate end, showing absence of triphosphates in the prepared poly I:C solution. Furthermore, IFN induction by poly I:C treated with RNase III for 60 min was not altered by additional treatment with RNase A for the removal of ssRNA contamination (unpublished data), indicating that RIG-I recognizes dsRNA without triphosphates, in addition to 5′-triphosphate ssRNAs. Collectively, these results suggest that the length of poly I:C determines the differential recognition by RIG-I and MDA5.

Differential regulation of ATPase activity by long and short poly I:C

It has been shown that RIG-I has the ability to catalyze ATP in the presence of dsRNA. To determine if this ATPase activity of these helicases is differentially activated by dsRNAs in a length-dependent manner, we examined the ATPase activity of purified RIG-I and MDA5 proteins in the presence of poly I:C or poly I:C treated with RNase III for 60 min (designated as short poly I:C). The ATPase activity of RIG-I increased in the presence of short poly I:C in a dose-dependent manner, and the activation was higher than that with untreated poly I:C. In contrast, untreated poly I:C strongly activated the ATPase activity of MDA5 compared with short poly I:C (Fig. 2 A), indicating that the ATPase activities of RIG-I and MDA5 are selectively activated by the short poly I:C and untreated long poly I:C, respectively. As expected, 5′-triphosphate ssRNA induced the ATPase activity of RIG-I, but not of MDA5 (Fig. 2 B). Thus, the ATPase activity clearly correlated with the IFN responses triggered by these RNA helicases, indicating that RIG-I and MDA5 directly distinguish between short and untreated long poly I:C molecules, respectively.

Association of poly I:C with RIG-I and MDA5

To investigate whether RIG-I and MDA5 directly distinguish between the lengths of poly I:C, we examined the binding of purified RIG-I and MDA5 proteins to poly I:C by atomic force microscope (AFM). As shown in Fig. 3 A, untreated poly I:C was detected as strings with lengths of 100–200 nm, and short poly I:C was visualized as dots (~1 nm high). MDA5 mixed with untreated poly I:C formed a thick structure indicated by bright white dots, representing the binding between MDA5 and poly I:C (Fig. 3 A). On the other hand, the mixture of RIG-I and untreated poly I:C failed to form such complexes. Reciprocally, short poly I:C mixed with RIG-I, but not MDA5, formed the thick structures. Next, we statistically analyzed the thickness of molecules visualized by AFM. Whereas the heights of poly I:C, short poly I:C, MDA5, or RIG-I alone were 0.5–1.5 nm, 2.5–5.5 nm structures appeared when poly I:C was mixed with MDA5, but not with RIG-I, protein (Fig. 3 B). In contrast, as shown in Fig. 3 C, an association of short poly I:C with RIG-I, but not with MDA5, was detected. These data indicate that RIG-I and MDA5 distinguish the lengths of poly I:C and specifically bind to their cognate ligands.

Differential recognition of short and long dsRNAs by two helicases

We examined if short dsRNAs other than poly I:C are also recognized by RIG-I. We chemically synthesized 70 base sense and antisense ssRNAs corresponding to the sequence of Lamin A/C harboring a 5′ hydroxyl end, annealed them, and examined their IFN-inducing ability. Whereas transfection of ssRNAs did not induce production of IFN-β, dsRNA generated by annealing sense and antisense ssRNAs (designated s and as in Fig. 4 A) induced IFN-β. Although the level of production was comparably low, it was clearly

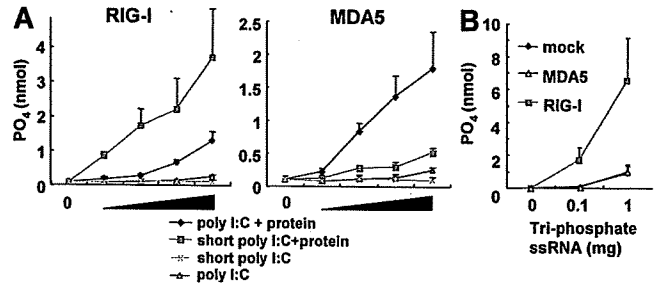

Figure 2. Long and short poly I:C preferentially activate ATPase activities of MDA5 and RIG-I. ATPase activity of RIG-I or MDA5 protein was measured in the presence of the indicated RNAs. The x axis shows the concentration of RNAs. (A) Long and short poly I:C. (B) 5′-tri-phosphate ssRNA. Several quantities (1, 0.2, 0.04, and 0.008 μg) of poly I:C were used. Error bars show SDs between triplicates.

Published June 30, 2008

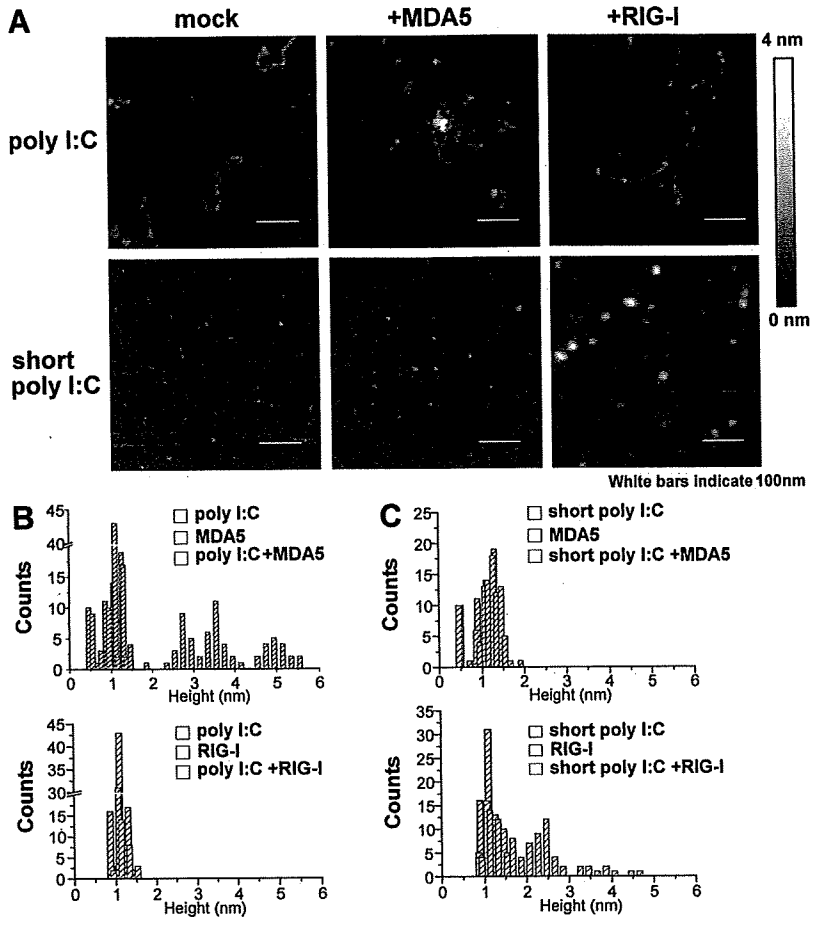

Figure 3. RIG-I and MDA5 specifically bind to short and long poly I:C. (A) Complex of indicated poly I:C and protein (MDA5 or RIG-I) was observed by AFM. Height is on a scale from 0 to 4 nm, with a low area depicted in dark brown and a higher area depicted in brighter color. Scale area, 500 nm. Bars, 100 nm. Those are representative images from several pictures. (B and C) Statistical height analyses of molecules corresponding to pictures in A.

dependent on RIG-I, indicating that a 70-bp dsRNA without 5′ triphosphate is also a RIG-I ligand (Fig. 4 A). To further analyze longer dsRNA synthesized in vitro by T7 polymerase in the production of IFN-β, we generated a 400 base sense and antisense ssRNA corresponding to the sequence of Lamin A/C harboring a 5′ capping with 7mG (designated s and as in Fig. 4 B). Introduction of dsRNA, generated by annealing capped 400 base sense and antisense ssRNAs, induced greatly enhanced RIG-I–dependent IFN-β production compared with the transfection of cells with each ssRNA (Fig. 4 B). These data also supported the aforementioned observation that dsRNA can induce IFN responses in a RIG-I–dependent fashion. We further examined the IFN responses triggered by 1–4 kbp capped-dsRNA. Although 1 kbp dsRNA-induced IFN-β was dependent on RIG-I, but not on MDA5, 2 kbp capped-dsRNA induced IFN-β, even in *Rig-I*$^{-/-}$ cells. The production of IFN-β in response to 3 and 4 kbp capped-dsRNA was less dependent on RIG-I, and an impairment of IFN-β production was observed in *Mda5*$^{-/-}$ cells (Fig. 4 C). Of note, *Rig-I*$^{-/-}$ *Mda5*$^{-/-}$ cells did not produce any IFN-β in response to 1–4 kbp capped-dsRNA (Fig. 4 C). These data indicate that RIG-I and MDA5 preferentially recognize short and long dsRNAs synthesized by T7 polymerase, respectively.

Recognition of viral genomic dsRNA by RIG-I and MDA5

We then examined whether viral dsRNAs are also differentially recognized by RIG-I and MDA5. Reovirus, a dsRNA virus, was used for further analysis. The production of IFN-β in response to reovirus was severely impaired in *Mda5*$^{-/-}$ conventional DCs (cDCs; Fig. 5 A), although this was totally abolished in *Rig-I* $^{-/-}$ *Mda5*$^{-/-}$ cDCs (not depicted). This result indicates that both RIG-I and MDA5 are involved in the recognition of reovirus, which is consistent with a recent study (24). Next, we stimulated MEFs with whole genomic RNA prepared from reovirus. Reovirus genome RNA induced production of IFN-β in either *Rig-I* $^{-/-}$ cells or *Mda5*$^{-/-}$ MEFs, but not in *Rig-I* $^{-/-}$ *Mda5*$^{-/-}$ MEFs (Fig. 5 B). These findings suggest that the reovirus genome RNA contains both RIG-I and MDA5 ligands. Reovirus genome RNA consists of 10 segments in three distinct classes called L, M, and S corresponding to their size. Segment sizes are 3.9 kbp (L), 2.2–2.3 kbp (M), and 1.2–1.4 kbp (S; Fig. 5 C). These fragments were purified from the whole reovirus genome and each fragment

Published June 30, 2008

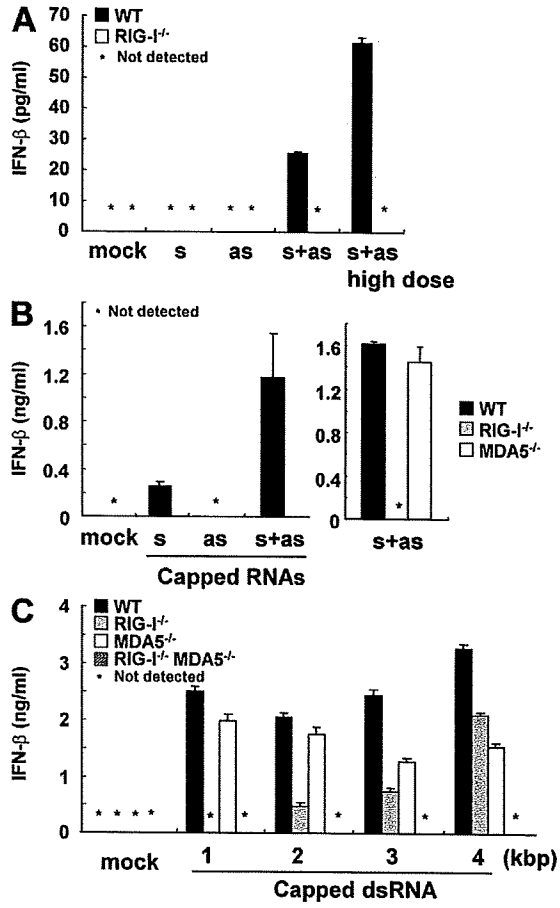

Figure 4. RIG-I and MDA5 selectively recognize dsRNA in a length-dependent manner. (A and B) Indicated genotype of MEFs were treated with 1 μg/ml of the indicated RNAs (10 μg/ml in the case of high dose) for 24 h. s, sense ssRNA; as, antisense ssRNA; s+as, dsRNA generated by annealing s with as. s and as are chemically synthesized 70-bp ssRNAs having a 5′ hydroxyl end in A. s and as are in vitro transcribed capped-ssRNAs in (B). The production of IFN-β in the supernatant was measured by ELISA. (C) WT, *Rig-I*$^{-/-}$, *Mda5*$^{-/-}$, and *Rig-I*$^{-/-}$*Mda5*$^{-/-}$ MEFs were treated with 1 μg/ml of in vitro–transcribed capped dsRNAs for 16 h. The production of IFN-β in the supernatant was measured by ELISA. Error bars show SDs between triplicates.

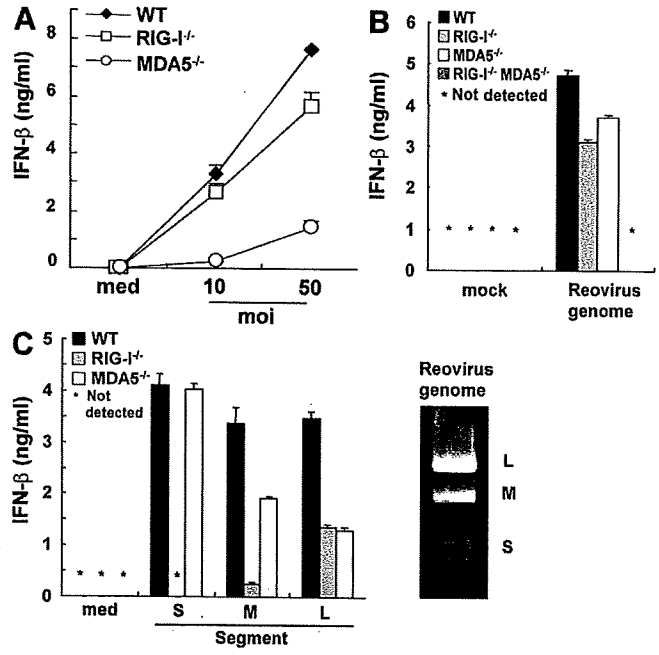

Figure 5. Reovirus genome dsRNA includes both RIG-I and MDA5 ligands. (A) WT, *Rig-I*$^{-/-}$, and *Mda5*$^{-/-}$ GM-CSF-DCs were infected with the indicated multiplicity of infection of reovirus. The production of IFN-β in the supernatant was measured by ELISA. (B and C) The indicated genotypes of MEFs were treated with 1 μg/ml of reovirus genome RNA (B) or 0.1 μg/ml of dsRNA segments (C) for 16 h. The production of IFN-β in the supernatant was measured by ELISA. The reoviral genome is shown on the ethidium bromide–stained gel (C, right), and the S (1.2–1.4 kbp), M (2.2–2.3 kbp), and L (3.9 kbp) segments are indicated. Error bars show SDs between triplicates.

was separately transfected into MEFs. As shown in Fig. 5 C, the production of IFN-β in response to S segments was dependent on RIG-I, but not on MDA5. The response to M fragments was not abrogated in *Rig-I*$^{-/-}$ MEFs, and was modestly impaired in *Mda5*$^{-/-}$ MEFs. In contrast, the production of IFN-β induced by L segments was reduced in both *Rig-I*$^{-/-}$ and *Mda5*$^{-/-}$ MEFs, suggesting that MDA5 contributed more to the recognition of longer segments of reovirus genomic dsRNA, whereas shorter segments were preferentially recognized by RIG-I.

MDA5 and RIG-I recognize viral dsRNA generated during replication

We have reported that EMCV is recognized by MDA5, whereas RIG-I detects VSV and influenza virus. In response to influenza virus infection, triphosphate ssRNA was considered to be the source of induction of type I IFNs, and no dsRNA was detectable during its replication (30, 33). To investigate whether triphosphate ssRNA is also the source of type I IFN induction in VSV infection, we harvested whole RNA from noninfected cells or virus-infected cells, and examined the IFN-β responses to the RNAs. RNA prepared from EMCV-infected cells induced IFN-β production in an MDA5-dependent manner (Fig. 6 A). Treatment of this RNA with calf intestine alkaline phosphatase (CIAP) did not reduce IFN-β production in MEFs (Fig. 6 B). In contrast, RNA from influenza virus–infected cells induced IFN-β production in a RIG-I–dependent manner, which was severely reduced after CIAP treatment (Fig. 6, A and B). IFN-β production in response to RNA from VSV-infected cells was dependent on RIG-I (Fig. 6 A) and this production was only partially reduced by treatment with CIAP (Fig. 6 B). These data suggest that 5′-triphosphate ssRNA is not the sole RIG-I ligand involved in VSV-induced IFN-β production. Furthermore, degradation of dsRNA from virus-infected cells by RNase III treatment abolished IFN-β–inducing activity in RNA from EMCV-infected cells (Fig. 6 B). Also the level of IFN production was impaired in RNA from VSV-infected cells by RNase III treatment, whereas the response to RNA from

Published June 30, 2008

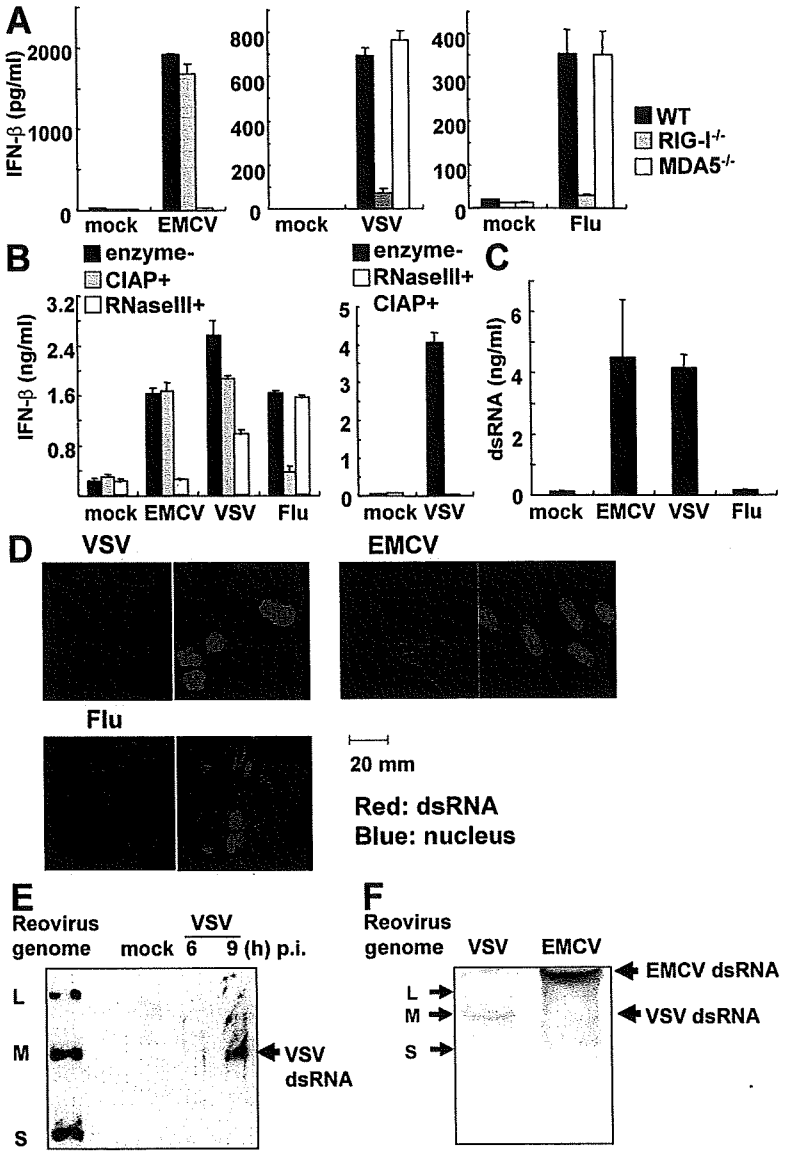

Figure 6. dsRNA generated during VSV replication induces IFNs in a RIG-I–dependent manner. (A) RNA samples harvested from uninfected (mock), EMCV-, VSV-, or influenza virus (flu)–infected cells were transfected into WT, *Rig-I*$^{-/-}$, and *Mda5*$^{-/-}$ MEFs. The production of IFN-β in the culture supernatant 10 h after transfection was measured by ELISA. (B) RNA harvested from noninfected (mock) or EMCV-, VSV-, or influenza virus–infected cells with CIAP-, RNase III-, both CIAP-, and RNase III-treatments or nontreatment (enzyme-) was transfected into WT MEFs. The production of IFN-β in the supernatant 10 h after transfection was measured by ELISA. (C) dsRNA in uninfected (mock), EMCV-, VSV-, or influenza virus–infected cells was measured by ELISA. (D) Immunostaining for dsRNA in MEFs infected with EMCV, VSV, and influenza virus for 8 h. Red, dsRNA; blue, nucleus. Error bars show SDs between triplicates. (E) RNA harvested from noninfected (mock) or VSV-infected cells (indicated periods) was electrophoresed in 1.5% agarose gel, transferred to a nylon membrane, and blotted by anti-dsRNA antibody. Reovirus genome RNAs were indicated as the size control. The arrow shows VSV dsRNA. (F) dsRNA blotting of RNA harvested from EMCV- or VSV-infected cells. RNAs were electrophoresed in nondenaturing 10% polyacrylamide gel. Reovirus genome RNAs were indicated (left). Arrows (right) show EMCV and VSV dsRNA.

influenza virus–infected cells was not altered after treatment. Moreover, treatment of RNA from VSV-infected cells with both CIAP- and RNase III abolished IFN-β–inducing activity (Fig. 6 B). These results further suggest that the dsRNA generated in VSV-infected cells is recognized by RIG-I to induce IFN-β production. To determine if dsRNA is generated during VSV infection, we performed quantification of dsRNA in viral-infected cells by ELISA. Interestingly, infection with VSV and EMCV produced high amounts of dsRNA, despite no dsRNA being detected after infection with influenza virus (Fig. 6 C). As shown in Fig. 6 D, dsRNA (red dot) was observed in EMCV-infected cells, but not in influenza virus–infected cells, consistent with previous reports (30, 33). The presence of dsRNA was also detected in VSV-infected cells (Fig. 6 D). These results suggest that dsRNA is generated in cells infected with VSV, a virus recognized by RIG-I,

Published June 30, 2008

and dsRNA, in addition to 5′-triphosphate ssRNA, might be a target for RIG-I–mediated recognition in vivo. On the other hand, long dsRNA could be generated in EMCV-infected cells and recognized by MDA5. Next, we examined the length of dsRNA generated after VSV infection. RNA harvested from cells infected with VSV for 6 or 9 h was electrophoresed, transferred to a nylon membrane, and blotted with anti-dsRNA antibody. As shown in Fig. 6 E, a dsRNA band was detected in the RNA sample (9-h infection of VSV), and the dsRNA migrated similar to M fragment of reovirus genomic RNA, suggesting that dsRNA generated in VSV infection is ~2.2 kbp. We compared the lengths of dsRNAs generated in VSV- and EMCV-infected cells. As shown in Fig. 6 E, dsRNA found in EMCV-infected cells was much longer than that detected in VSV-infected cells. Although it is difficult to determine precise length of dsRNAs, the dsRNA from EMCV-infected cells migrated much slower than the L fragment of reovirus genomic RNA (3.9 kbp). These data suggest that the lengths of dsRNAs generated in RNA virus-infected cells varied depending on the virus species, and this difference could explain the differential recognition of viruses by RIG-I and MDA5.

DISCUSSION

Our data indicate that RIG-I recognizes dsRNA in addition to 5′-triphosphate end ssRNA, and the length of dsRNA determines the utilization of RIG-I and MDA5 for the recognition. Genomic dsRNAs of Reovirus are also differentially recognized by RIG-I and MDA5 depending on the length of the dsRNA. The results also indicate that VSV, a rhabdovirus recognized by RIG-I, generates dsRNA in infected cells, whereas influenza virus does not generate dsRNA in the cells as reported previously (33).

The 5′-triphosphate ssRNA has been considered to be the sole ligand for RIG-I because dsRNA has been generated in vitro by a T7 polymerase using nucleotide-triphosphates as substrates (34). However, we discovered that RNase III-treated short poly I:C is another RIG-I ligand (Fig. 1). Poly I:C, a synthetic MDA5 ligand, was converted to a RIG-I ligand, when the length of dsRNA was shortened. The 5′ ends of short poly I:C harbor either monophosphate or diphosphate, showing that dsRNA without triphosphate is also a RIG-I ligand. RNase III and Dicer are dsRNA specific endonucleases generating 15–25 nt short dsRNAs, which mediate RNAi in a cell. Indeed, completely digested poly I:C lost the activity to induce type I IFNs, indicating that a certain length of dsRNA is required for RIG-I–mediated recognition. It was reported that host RNA digested by RNase L could be recognized by RIG-I for inducing IFN-β (35). Although it is not clear if the RNase L-digested RNA could harbor 5′-triphosphate for activating immune cells, the length of RNA might be important for RIG-I–mediated recognition in RNA digested with RNase L. Furthermore, chemically synthesized RNAs which do not possess a phosphate at the 5′ end also stimulated cells in a RIG-I–dependent manner, clearly indicating that dsRNA elicits RIG-I–mediated IFN responses independent of 5′-triphosphate. The amount of IFN-β produced in response to synthetic 70 nt dsRNA was lower than that in response to 5′ triphosphate end ssRNA and short poly I:C. It may be possible that 70 nt dsRNA is not long enough to efficiently induce IFN-β in MEFs. Alternatively, the presence of mono- or diphosphate at the 5′ end of dsRNAs might enhance recognition by RIG-I.

We also clarified that MDA5 and RIG-I directly distinguish between long and short dsRNAs generated by T7 polymerase in the presence of 7mG. ~1 kbp dsRNAs induced IFNs in a RIG-I–dependent manner. ~2 kbp dsRNAs induced IFNs even in RIG-I–deficient cells, and the induction was MDA5 dependent, showing that MDA5 preferentially recognizes long dsRNAs and RIG-I is involved in the recognition of short dsRNAs. This explains why poly I:C is an MDA5 ligand and poly I:C is shifted from being an MDA5 ligand to being a RIG-I ligand, after shortening of the length of dsRNA by RNase III treatment. Also, our data indicate that viral short and long dsRNA are also differentially recognized by RIG-I and MDA5. Reovirus genome RNA contains several lengths of dsRNA fragments and long dsRNA fragments induced IFN production in an MDA5-dependent manner, whereas IFN induction by short dsRNAs was RIG-I dependent. These data indicate that MDA5 and RIG-I differentiate between the lengths of dsRNA and the mechanism of how these helicases distinguish the length is an interesting issue.

Long and short poly I:C distinctly activated the ATPase activity of MDA5 and RIG-I, respectively. The ATPase activity was found to correlate with biological IFN responses triggered by these RNA helicases, suggesting that the induction of ATPase activity is the key to revealing the mechanism of how RIG-I and MDA5 recognize viral RNA and transduce signaling to downstream molecules. In addition to dsRNAs, triphosphate ssRNA activates the ATPase activity of RIG-I, but not of MDA5, suggesting that this ATPase activity is necessary not just for unwinding dsRNAs. Thus, the ATPase activity might be essential for conformational changes of these helicases to signal downstream, such as opening the CARD position masked by their helicases and RD domains. Whether this ATPase activity correlates with conformational changes of RIG-I and MDA5 remains to be determined and structural analysis of these helicases is desirable. Furthermore, we observed, with AFM, the specific association of MDA5 with poly I:C and also of RIG-I with the short poly I:C. It is interesting that the binding of these helicases to dsRNA also correlates with the biological IFN responses triggered by these RNA helicases. The mechanism of how these two helicases distinguish the length of dsRNA, leading to the specific binding to dsRNAs is an exciting issue for future studies.

Using *Mda5*$^{-/-}$ and *Rig-I*$^{-/-}$ mice, it has been shown that poly I:C is preferentially detected by MDA5 in inducing type I IFNs, and the contribution of RIG-I in poly I:C recognition was low (26). However, several reports showed that RIG-I was also involved in poly I:C recognition in vitro. Overexpression of RIG-I in cell lines activates an IFN-β promoter and its activation level is clearly augmented by poly

Published June 30, 2008

JEM

I:C stimulation. RIG-I, as well as MDA5, is shown to bind to poly I:C (23). We tested poly I:Cs purchased from several companies and found that the induction of IFNs by some poly I:Cs was impaired in *Rig-I*$^{-/-}$ cells when the size of these poly I:Cs was comparably small (unpublished data). These observations are also consistent with our conclusion that the length of poly I:C is important for the differential recognition by RIG-I and MDA5.

Neither dsRNA nor 5′ triphosphate end RNA are present in the cytoplasm of host resting cells, and these RNA structures are the target of recognition by innate immunity. In response to RNA virus infection, dsRNA is generated in the course of viral RNA replication. However, it was also shown that dsRNA is barely present in infected cells, and 5′ triphosphate RNA was shown to be the major target of recognition. Indeed, dsRNA was not detected in influenza virus infected cells as shown previously (33). Consistently, IFN-β production in response to RNA from influenza virus–infected cells depended on the presence of the 5′-triphosphate end as determined by CIAP treatment. On the other hand, EMCV and VSV generated dsRNA in the cells, which were recognized by MDA5 and RIG-I, respectively. RNase III treatment of RNAs from VSV-infected cells impaired the IFN-β–inducing activity, indicating that dsRNA, generated in the course of VSV infection, contributed to RIG-I–mediated recognition. As reported previously, dsRNA generated by EMCV infection appears to be responsible for MDA5-mediated recognition. The length of dsRNA generated by VSV appeared to be close to 2.0–2.5 kbp by the immunoblot analysis with anti-dsRNA antibody. Given that the length of VSV genomic RNA is 11 kb, the dsRNA was not the replication intermediate of VSV. It has been reported that defective interfering (DI) particles are generated in VSV-infected cells, and the size of reported DI particles is ∼2.2 kb (36). Thus, dsRNA generated in the course of VSV replication might be derived from DI particles, although further studies are needed to clarify what is the source of the dsRNA. On the other hand, dsRNA found in EMCV–infected cells was much longer than that detected in VSV-infected cells. This long dsRNA is assumed as the replication intermediates of EMCV genomic RNA (∼8 kb); however, the characteristic of dsRNA generated by EMCV remains to be determined. These data suggest that MDA5 and RIG-I distinctly recognize long and short dsRNAs generated in a cell after RNA virus infection. RNA viruses recognized by RIG-I could possibly be subclassified based on the contribution of 5′-triphosphate end ssRNA and short dsRNA. In the future, it would be interesting to explore if the lengths of dsRNA differ between several RNA viruses recognized by RIG-I and MDA5.

In summary, we characterized the RNA molecules recognized by RIG-I and MDA5, and showed that dsRNAs differentially induce RIG-I– and MDA5-mediated IFN responses depending on length. Viral RNAs were also differentially recognized by RIG-I and MDA5, suggesting that the two helicases evolved for covering a broad spectrum of RNA viruses. The identification of the nature of dsRNA recognition will lead to the discovery of small molecules efficiently activating RIG-I and/or MDA5, and will lead to the development of novel vaccines and therapies against viral infection.

MATERIALS AND METHODS

Cells and viruses. *Mda5*$^{-/-}$ and *Rig-I*$^{-/-}$ MEFs and GM-CSF DCs were generated as previously described (26, 37). EMCV, influenza virus, and VSV were obtained as previously described (26). Reovirus was as previously described (38).

Purification of recombinant RIG-I and MDA5. RIG-I protein was purified as previously described (24). For the synthesis of MDA5, 2xFlag-$MDA5_{2\text{-}1025}$ (MDA5) was expressed as a GST-fusion protein using a BaculoGold GST-Expression System (BD Biosciences). GST-MDA5 bound to Glutathione–Sepharose 4B (GE Healthcare) was eluted by digestion with AcTEV protease (Invitrogen) and passed through Ni-NTA Agarose (QIAGEN). MDA5 was further purified by Q-Sepharose (GE Healthcare) chromatography.

ATPase assays. ATPase assays were performed in 25 μl of ATPase reaction buffer (20 mM Tris-HCl, pH 8.0, 1.5 mM $MgCl_2$, and 1.5 mM DTT) including 1 μg of purified RIG-I or MDA5 protein and the indicated amounts of RNAs (tri-p-ssRNA, etc.). After a 15-min incubation at 37°C, 50 nmol of ATP was added and the mixture was further incubated at 37°C for 1 h. BIOMOL GREEN Reagent (BIOMOL) was added for 5 min, and the absorbance at 620 nm was determined.

Immunofluorescence analysis. MEFs were infected with the indicated virus for 8 h and fixed with 4% paraformaldehyde. Cells were then permeabilized with 0.5% Triton X-100 dissolved in PBS. For the detection of dsRNA, the mouse monoclonal antibody J2 and Alexa Fluor 594 anti–mouse secondary antibody (Invitrogen) were used.

Sample solution for AFM imaging. RNAs and proteins were diluted with sterile purified water to the final concentration of 25 ng/μl and 2.5 ng/μl, respectively. Each solution was incubated for 30 min at room temperature.

AFM imaging. 5 μl of each sample solution was dropped on freshly cleaved mica (Nilaco). After 1 min, the mica surface was rinsed with 100 μl of sterile purified water and dried in air. AFM observation was performed using a commercial microscope operating in the dynamic force mode (model SPI3700-SPA300; Seiko) with an Si micro-cantilever (model SI-DF20; Seiko; spring constant = 15 N/m, resonance frequency = 135 kHz) (39). AFM images were analyzed using the SPIP Metrology software package (Image Metrology).

Preparation of RNAs. Uncapped in vitro–transcribed dsRNA, capped RNAs, and 5′-triphosphate ssRNA were synthesized using a T7 RiboMAX Express RNAi System (Promega), the T7 Megascript Ultra kit (Ambion; 7mGpppG/GTP ratio of 8:1), and Silencer siRNA Construction kit (Ambion), respectively, following the manufacturers' instructions. Depending on the case, poly I:C was generated in vitro using PNPase with IDP or CDP. CIAP (TaKaRa) treatment was performed as previously described (29). Processing of poly I:C (GE Healthcare) was performed in 10 μl reaction buffer containing 2 μl of 5x buffer (siRNaseIII; TaKaRa), 2.5 mM $MgCl_2$, 10 μg of poly I:C, and 1 U of RNaseIII, for the indicated periods, and the reaction was stopped by 2 μl of 120 mM EDTA. RNase A and Bal31 (TaKaRa) treatment was performed according to the manufacturer's instructions. Chemically synthesized ssRNAs (70 base) with a 5′ hydroxyl were purchased from Gene Design, Inc.

Preparation of viral RNAs. Vero cells plated on 20 × 15-cm dishes were infected with multiplicity of infection 0.01 of reovirus. At 1 h after infection, medium was removed and replaced with DME containing 10% FCS and the cells were incubated for 2 d at 37°C. Then the supernatants were collected and centrifuged at 3,000 rpm for 15 min to remove cells for avoiding cellar

Published June 30, 2008

RNA contamination. The supernatants were harvested and centrifuged at 25,000 rpm for 90 min in an SW28 rotor at 4°C. The viral pellet was suspended in TRIzol reagent (Invitrogen) and RNA was extracted. 30 μg of reovirus RNA was obtained.

ELISA. The amount of dsRNA in viral-infected MEFs was determined by sandwich ELISA (30) using the mAb K1 as the capture antibody and biotinylated mAb J2 for detection, followed by streptavidin alkaline phosphatase. A 400-bp in vitro–transcribed dsRNA was used as a standard to calculate dsRNA concentrations. ELISA for IFN-β was performed as previously described (26).

dsRNA blot. RNA harvested from noninfected, VSV-, or EMCV-infected cells (20 μg) was electrophoresed in 1.5% agarose gel or 10% nondenaturing polyacrylamide gel, transferred to a nylon membrane (Hybond N+), blotted with mouse anti-dsRNA antibody (J2; English and Scientific Consulting) and visualized with an enhanced chemiluminescence system (PerkinElmer). Reovirus genome RNAs were electrophoresed in the same gel and indicated as the size control.

Online supplemental material. Fig. S1 shows IFN-β production from GM-CSF–induced WT, *RIG-I*$^{-/-}$, and *MDA5*$^{-/-}$ cDCs in the stimulation with poly I:C or short poly I:C (1 μg/ml). Fig. S2 shows IFN-β production in sera of mice 6 h after intravenous injection of 20 μg poly I:C or short poly I:C. The online version of this article is available at http://www.jem.org/cgi/content/full/jem.20080091/DC1.

The authors wish to thank Y. Fujiwara, M. Shiokawa, and N. Kitagaki for technical assistance and M. Hashimoto for secretarial assistance.

This work was supported in part by grants from the Ministry of Education, Culture, Sports, Science and Technology in Japan; from the Ministry of Health, Labour and Welfare in Japan; from the 21st Century Center of Excellence Program of Japan; and from the National Institutes of Health (AI070167).

The authors have no financial conflict of interests.

Submitted: 14 January 2008
Accepted: 4 June 2008

REFERENCES

1. Akira, S., S. Uematsu, and O. Takeuchi. 2006. Pathogen recognition and innate immunity. *Cell.* 124:783–801.
2. Beutler, B., C. Eidenschenk, K. Crozat, J.L. Imler, O. Takeuchi, J.A. Hoffmann, and S. Akira. 2007. Genetic analysis of resistance to viral infection. *Nat. Rev. Immunol.* 7:753–766.
3. Medzhitov, R. 2007. Recognition of microorganisms and activation of the immune response. *Nature.* 449:819–826.
4. Fujita, T., K. Onoguchi, K. Onomoto, R. Hirai, and M. Yoneyama. 2007. Triggering antiviral response by RIG-I-related RNA helicases. *Biochimie.* 89:754–760.
5. Alexopoulou, L., A.C. Holt, R. Medzhitov, and R.A. Flavell. 2001. Recognition of double-stranded RNA and activation of NF-kappaB by Toll-like receptor 3. *Nature.* 413:732–738.
6. Diebold, S.S., T. Kaisho, H. Hemmi, S. Akira, and C. Reis e Sousa. 2004. Innate antiviral responses by means of TLR7-mediated recognition of single-stranded RNA. *Science.* 303:1529–1531.
7. Heil, F., H. Hemmi, H. Hochrein, F. Ampenberger, C. Kirschning, S. Akira, G. Lipford, H. Wagner, and S. Bauer. 2004. Species-specific recognition of single-stranded RNA via toll-like receptor 7 and 8. *Science.* 303:1526–1529.
8. Hemmi, H., O. Takeuchi, T. Kawai, T. Kaisho, S. Sato, H. Sanjo, M. Matsumoto, K. Hoshino, H. Wagner, K. Takeda, and S. Akira. 2000. A Toll-like receptor recognizes bacterial DNA. *Nature.* 408:740–745.
9. Adachi, O., T. Kawai, K. Takeda, M. Matsumoto, H. Tsutsui, M. Sakagami, K. Nakanishi, and S. Akira. 1998. Targeted disruption of the MyD88 gene results in loss of IL-1- and IL-18-mediated function. *Immunity.* 9:143–150.
10. Yamamoto, M., S. Sato, H. Hemmi, K. Hoshino, T. Kaisho, H. Sanjo, O. Takeuchi, M. Sugiyama, M. Okabe, K. Takeda, and S. Akira. 2003. Role of adaptor TRIF in the MyD88-independent toll-like receptor signaling pathway. *Science.* 301:640–643.
11. Liu, Y.J. 2005. IPC: professional type 1 interferon-producing cells and plasmacytoid dendritic cell precursors. *Annu. Rev. Immunol.* 23:275–306.
12. Yoneyama, M., M. Kikuchi, T. Natsukawa, N. Shinobu, T. Imaizumi, M. Miyagishi, K. Taira, S. Akira, and T. Fujita. 2004. The RNA helicase RIG-I has an essential function in double-stranded RNA-induced innate antiviral responses. *Nat. Immunol.* 5:730–737.
13. Andrejeva, J., K.S. Childs, D.F. Young, T.S. Carlos, N. Stock, S. Goodbourn, and R.E. Randall. 2004. The V proteins of paramyxoviruses bind the IFN-inducible RNA helicase, mda-5, and inhibit its activation of the IFN-beta promoter. *Proc. Natl. Acad. Sci. USA.* 101:17264–17269.
14. Rothenfusser, S., N. Goutagny, G. Diperna, M. Gong, B.G. Monks, A. Schoenemeyer, M. Yamamoto, S. Akira, and K.A. Fitzgerald. 2005. The RNA helicase Lgp2 inhibits TLR-independent sensing of viral replication by retinoic acid-inducible gene-I. *J. Immunol.* 175:5260–5268.
15. Kawai, T., K. Takahashi, S. Sato, C. Coban, H. Kumar, H. Kato, K.J. Ishii, O. Takeuchi, and S. Akira. 2005. IPS-1, an adaptor triggering RIG-I- and Mda5-mediated type I interferon induction. *Nat. Immunol.* 6:981–988.
16. Kumar, H., T. Kawai, H. Kato, S. Sato, K. Takahashi, C. Coban, M. Yamamoto, S. Uematsu, K.J. Ishii, O. Takeuchi, and S. Akira. 2006. Essential role of IPS-1 in innate immune responses against RNA viruses. *J. Exp. Med.* 203:1795–1803.
17. Seth, R.B., L. Sun, C.K. Ea, and Z.J. Chen. 2005. Identification and characterization of MAVS, a mitochondrial antiviral signaling protein that activates NF-kappaB and IRF 3. *Cell.* 122:669–682.
18. Sun, Q., L. Sun, H.H. Liu, X. Chen, R.B. Seth, J. Forman, and Z.J. Chen. 2006. The specific and essential role of MAVS in antiviral innate immune responses. *Immunity.* 24:633–642.
19. Meylan, E., J. Curran, K. Hofmann, D. Moradpour, M. Binder, R. Bartenschlager, and J. Tschopp. 2005. Cardif is an adaptor protein in the RIG-I antiviral pathway and is targeted by hepatitis C virus. *Nature.* 437:1167–1172.
20. Xu, L.G., Y.Y. Wang, K.J. Han, L.Y. Li, Z. Zhai, and H.B. Shu. 2005. VISA is an adapter protein required for virus-triggered IFN-beta signaling. *Mol. Cell.* 19:727–740.
21. Sato, M., H. Suemori, N. Hata, M. Asagiri, K. Ogasawara, K. Nakao, T. Nakaya, M. Katsuki, S. Noguchi, N. Tanaka, and T. Taniguchi. 2000. Distinct and essential roles of transcription factors IRF-3 and IRF-7 in response to viruses for IFN-alpha/beta gene induction. *Immunity.* 13:539–548.
22. Honda, K., H. Yanai, H. Negishi, M. Asagiri, M. Sato, T. Mizutani, N. Shimada, Y. Ohba, A. Takaoka, N. Yoshida, and T. Taniguchi. 2005. IRF-7 is the master regulator of type-I interferon-dependent immune responses. *Nature.* 434:772–777.
23. Yoneyama, M., M. Kikuchi, K. Matsumoto, T. Imaizumi, M. Miyagishi, K. Taira, E. Foy, Y.M. Loo, M. Gale Jr., S. Akira, et al. 2005. Shared and unique functions of the DExD/H-Box helicases RIG-I, MDA5, and LGP2 in antiviral innate immunity. *J. Immunol.* 175:2851–2858.
24. Saito, T., R. Hirai, Y.M. Loo, D. Owen, C.L. Johnson, S.C. Sinha, S. Akira, T. Fujita, and M. Gale Jr. 2007. Regulation of innate antiviral defenses through a shared repressor domain in RIG-I and LGP2. *Proc. Natl. Acad. Sci. USA.* 104:582–587.
25. Venkataraman, T., M. Valdes, R. Elsby, S. Kakuta, G. Caceres, S. Saijo, Y. Iwakura, and G.N. Barber. 2007. Loss of DExD/H box RNA helicase LGP2 manifests disparate antiviral responses. *J. Immunol.* 178:6444–6455.
26. Kato, H., O. Takeuchi, S. Sato, M. Yoneyama, M. Yamamoto, K. Matsui, S. Uematsu, A. Jung, T. Kawai, K.J. Ishii, et al. 2006. Differential roles of MDA5 and RIG-I helicases in the recognition of RNA viruses. *Nature.* 441:101–105.
27. Loo, Y.M., J. Fornek, N. Crochet, G. Bajwa, O. Perwitasari, L. Martinez-Sobrido, S. Akira, M.A. Gill, A. Garcia-Sastre, M.G. Katze, and M. Gale Jr. 2008. Distinct RIG-I and MDA5 signaling by RNA viruses in innate immunity. *J. Virol.* 82:335–345.

Published June 30, 2008

28. Gitlin, L., W. Barchet, S. Gilfillan, M. Cella, B. Beutler, R.A. Flavell, M.S. Diamond, and M. Colonna. 2006. Essential role of mda-5 in type I IFN responses to polyriboinosinic:polyribocytidylic acid and encephalomyocarditis picornavirus. *Proc. Natl. Acad. Sci. USA.* 103:8459–8464.
29. Hornung, V., J. Ellegast, S. Kim, K. Brzozka, A. Jung, H. Kato, H. Poeck, S. Akira, K.K. Conzelmann, M. Schlee, et al. 2006. 5′-triphosphate RNA is the ligand for RIG-I. *Science.* 314:994–997.
30. Pichlmair, A., O. Schulz, C.P. Tan, T.I. Naslund, P. Liljestrom, F. Weber, and C. Reis e Sousa. 2006. RIG-I-mediated antiviral responses to single-stranded RNA bearing 5′-phosphates. *Science.* 314:997–1001.
31. Marques, J.T., T. Devosse, D. Wang, M. Zamanian-Daryoush, P. Serbinowski, R. Hartmann, T. Fujita, M.A. Behlke, and B.R. Williams. 2006. A structural basis for discriminating between self and nonself double-stranded RNAs in mammalian cells. *Nat. Biotechnol.* 24:559–565.
32. Grunberg-Manago, M., P.J. Oritz, and S. Ochoa. 1955. Enzymatic synthesis of nucleic acidlike polynucleotides. *Science.* 122:907–910.
33. Weber, F., V. Wagner, S.B. Rasmussen, R. Hartmann, and S.R. Paludan. 2006. Double-stranded RNA is produced by positive-strand RNA viruses and DNA viruses but not in detectable amounts by negative-strand RNA viruses. *J. Virol.* 80:5059–5064.
34. Kim, D.H., M. Longo, Y. Han, P. Lundberg, E. Cantin, and J.J. Rossi. 2004. Interferon induction by siRNAs and ssRNAs synthesized by phage polymerase. *Nat. Biotechnol.* 22:321–325.
35. Malathi, K., B. Dong, M. Gale Jr., and R.H. Silverman. 2007. Small self-RNA generated by RNase L amplifies antiviral innate immunity. *Nature.* 448:816–819.
36. Pattnaik, A.K., L.A. Ball, A. LeGrone, and G.W. Wertz. 1995. The termini of VSV DI particle RNAs are sufficient to signal RNA encapsidation, replication, and budding to generate infectious particles. *Virology.* 206:760–764.
37. Kato, H., S. Sato, M. Yoneyama, M. Yamamoto, S. Uematsu, K. Matsui, T. Tsujimura, K. Takeda, T. Fujita, O. Takeuchi, and S. Akira. 2005. Cell type-specific involvement of RIG-I in antiviral response. *Immunity.* 23:19–28.
38. Connolly, J.L., and T.S. Dermody. 2002. Virion disassembly is required for apoptosis induced by reovirus. *J. Virol.* 76:1632–1641.
39. Mikamo, E., C. Tanaka, T. Kanno, H. Akiyama, G. Jung, H. Tanaka, and T. Kawai. 2005. Native polysomes of Saccharomyces cerevisiae in liquid solution observed by atomic force microscopy. *J. Struct. Biol.* 151:106–110.